



## **Local absorption of uncertainty in complex systems using resilient objects**

Downloaded from: <https://research.chalmers.se>, 2025-12-04 22:48 UTC

Citation for the original published paper (version of record):

Panarotto, M., Alonso Fernandez, I. (2024). Local absorption of uncertainty in complex systems using resilient objects. *Journal of Engineering Design*, 35(10): 1292-1310.  
<http://dx.doi.org/10.1080/09544828.2024.2327913>

N.B. When citing this work, cite the original published paper.



## Local absorption of uncertainty in complex systems using resilient objects

Massimo Panarotto & Iñigo Alonso Fernández

**To cite this article:** Massimo Panarotto & Iñigo Alonso Fernández (15 Mar 2024): Local absorption of uncertainty in complex systems using resilient objects, Journal of Engineering Design, DOI: [10.1080/09544828.2024.2327913](https://doi.org/10.1080/09544828.2024.2327913)

**To link to this article:** <https://doi.org/10.1080/09544828.2024.2327913>



© 2024 The Author(s). Published by Informa UK Limited, trading as Taylor & Francis Group.



Published online: 15 Mar 2024.



Submit your article to this journal [↗](#)



Article views: 203





View related articles [↗](#)



View Crossmark data [↗](#)

# Local absorption of uncertainty in complex systems using resilient objects

Massimo Panarotto <sup>a,b</sup> and Iñigo Alonso Fernández <sup>a</sup>

<sup>a</sup>Department of Industrial and Materials Science, Chalmers University of Technology, Gothenburg, Sweden;

<sup>b</sup>Department of Mechanical Engineering, Politecnico di Milano, Milano, Italy

## ABSTRACT

Traditional approaches to managing uncertainties during product development often lead to increased complexity and resource consumption. This paper introduces the concept of ‘resilient objects’ as an alternative solution, designed to provide passive protection against disruptive events of different kinds, thereby reducing the necessity for complex margins at system interfaces. The paper illustrates the concept of resilient objects through practical examples, which demonstrate the objects’ ability to uphold system functionality even when faced with unexpected disruptive events. By embodying resilience locally in areas of the system that are most susceptible to uncertain conditions, resilient objects offer the potential to minimise interface margins and thus the need for excessive system over-design. The concept of resilient objects offers a new perspective on how to solve the trade-offs between resilience and complexity when addressing uncertainties in the dynamic landscape of product development.

## ARTICLE HISTORY

Received 13 February 2023

Accepted 4 March 2024

## KEYWORDS

Resilient objects; uncertainty management; engineering design; complexity trade-offs; disruptive events

## Introduction

Most products traditionally evolve from prior products (Suh et al. 2010). However, this approach is now challenged due to growing uncertainties in market and technology, some of which are unknown (Brahma et al. 2023). For example, new groundbreaking technologies are emerging and expected to be integrated into products to meet customer and societal demands. However, the timing and impact of these introductions remain unclear. Simultaneously, ‘circular economy’ business models (Stahel 2016) encourage repurposing existing systems (Eckert, Isaksson, and Earl 2019). For instance, a car’s cooling system could find a new life in a greenhouse, but the original designers may not anticipate such applications or their unique environmental conditions, leading to missed repurposing opportunities.

These examples stress the need for systems that can withstand uncertainties, both known and unknown. Several design strategies address this challenge, including: (1) using standardised interfaces to facilitate component replacement (Ulrich 1995), (2) enabling rapid system repair (Hosseini, Barker, and Ramirez-Marquez 2016; Koh 2022), and (3)

**CONTACT** Massimo Panarotto  [massimo.panarotto@chalmers.se](mailto:massimo.panarotto@chalmers.se)  Department of Industrial and Materials Science, Chalmers University of Technology, Chalmersplatsen 4, 412 96, Gothenburg, Sweden

© 2024 The Author(s). Published by Informa UK Limited, trading as Taylor & Francis Group.

This is an Open Access article distributed under the terms of the Creative Commons Attribution License (<http://creativecommons.org/licenses/by/4.0/>), which permits unrestricted use, distribution, and reproduction in any medium, provided the original work is properly cited. The terms on which this article has been published allow the posting of the Accepted Manuscript in a repository by the author(s) or with their consent.

introducing margins to prevent change propagation throughout the system. While effective, these strategies often increase complexity across the product lifecycle, including the product, process, and organisation (Eckert, Isaksson, and Earl 2019; Jones and Eckert 2023).

This paper presents an alternative approach to ensure protection against uncertainties while keeping the system as simple as possible. We propose designing general-purpose ‘resilient objects’ capable of absorbing various disruptive events of different kinds and placing them in the regions of the product that are most susceptible to uncertain conditions. Such objects, like spring-damper systems, are already common in practice, such as suspensions in a car. This paper introduces a method for modeling and analyzing the impact of such general-purpose resilient objects.

## Background and core concepts

This paper focuses on ‘resilience’ for several reasons. Resilience is often defined as a system’s ability to ‘return to its original (or desired) state after being disturbed’ (Christopher and Rutherford 2004) and its capacity to ‘bounce back from adversity’ (Hollnagel, Nemeth, and Dekker 2008). Although there is an increasing number of publications on resilience (e.g. Hosseini, Barker, and Ramirez-Marquez 2016), there remains a lack of clarity regarding the ‘designerly ways’ (Cross 2006) to achieve resilience (Wied, Oehmen, and Welo 2020). Some general design principles to achieve resilience are:

- By possessing reserves to accommodate unforeseen changes (Hollnagel & al., 2008; Guo et al. 2023).
- By absorbing and utilise change (Uday and Marais 2015).
- By recovering from perturbation (Yodo and Wang 2016).
- By preventing adverse events (Guo et al. 2023).

Looking at these general principles, one can notice why the notion of resilience is often confused with similar strategies including reliability, robustness, adaptability, versatility, resilience, and flexibility. This lack of clarity makes it difficult to systematically use these concepts during design. In the field of engineering design, Chalupnik, Wynn, and Clarkson (2013) made a classification based on the point of view that such ‘ilities’ are providing different forms of system reliability (i.e. minimising unwanted variance in performance’; Zimmermann et al. 2017). According to Chalupnik, Wynn, and Clarkson (2013), a resilient design emphasises *passive protection* against uncertainty, in contrast to *active protection* (which characterises flexible systems instead). Active protection involves a system’s ability to adapt its structure to handle unknowns. In contrast, passive protection allows the system to address uncertain situations without altering its structure or configuration. An example of a flexible design is variable wing geometries in an aircraft (Chalupnik, Wynn, and Clarkson 2013), as they enable the modification of aerodynamic properties by changing the wing’s structure (i.e. by applying active protection). While such flexible design offers protection against uncertainty, it also introduces complexity, such as the need for actuators to enable wing geometry changes.

Conversely, a resilient design focuses on passive protection against uncertainty, potentially leading to reduced complexity. The benefits of this approach are detailed in the following section, where we introduce the concept of ‘resilient objects’ through an illustrative example.

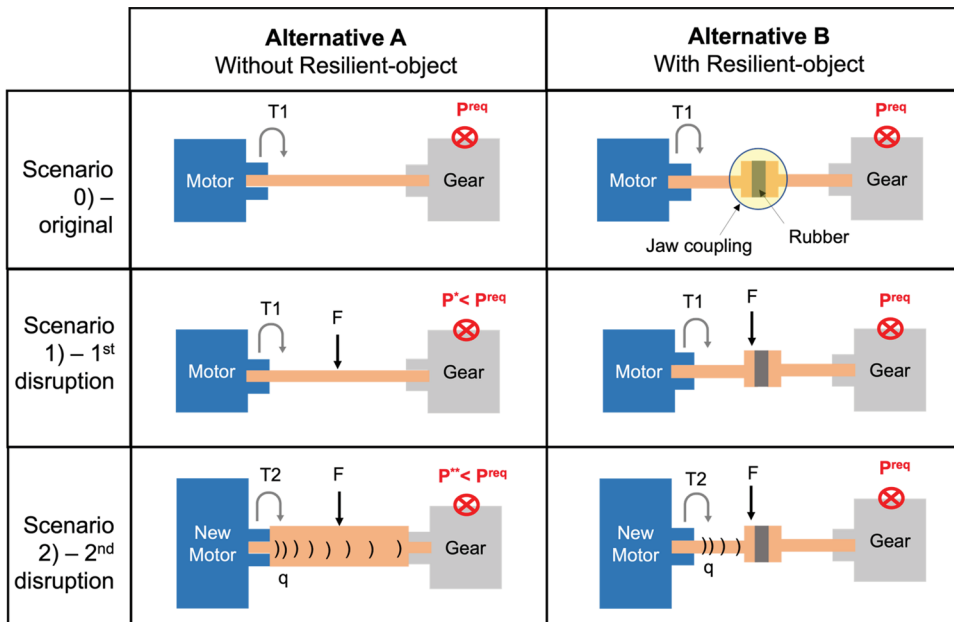


**Figure 1.** Comparison between two motor-shaft-gear system alternatives subject to two disruptive events (scenario 1 and scenario 2). In Alternative B, a jaw coupling is used as ‘resilient object’ to absorb uncertainty without altering the system configuration.

### *Illustrative example: a jaw coupling as a resilient object*

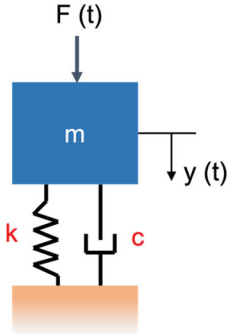
The example pertains to a jaw coupling (Figure 1), a versatile power transmission element designed to transmit torque between two shafts. Additionally, it dampens system vibrations and compensates for misalignment, thus safeguarding other components from potential damage. A jaw coupling comprises three components: two metallic hubs and an elastomeric element (commonly ‘rubber’) placed between the hubs, often referred to as a ‘spider.’ These three parts are assembled through a press fit, with one jaw from each hub alternating with the lobes of the spider.

Figure 1 illustrates the jaw coupling as a ‘resilient object,’ capable of passively addressing multiple disruptive events stemming from uncertainty. In the ‘original’ scenario (Scenario 0), two alternatives are explored:

In Alternative A, an idealised motor-shaft-gear system is considered, where the primary system function is to provide a specified force  $P^{req}$  (orthogonal to the figure) at the gear teeth contact. Alternative B replicates the same system but includes the jaw coupling situated between two shafts.

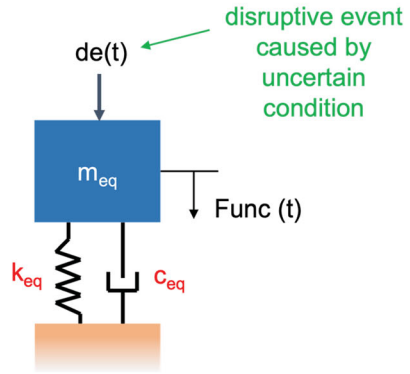
A new unexpected disruptive event (Scenario 1) introduces an additional load ( $F$ ) applied in the middle of the shaft. This extra load leads to adverse effects, such as shaft misalignment, which reduces the force at the gear teeth contact ( $P^* < P^{req}$ ). In Alternative A, this can be addressed by replacing the shaft with a larger cross-sectioned one, eliminating misalignment but necessitating the disposal of the old shaft. In Alternative B, the jaw coupling can absorb the misalignment without altering the overall structure.

## Mass-spring-damper



$$m \frac{d^2 y}{dt^2} + c \frac{dy}{dt} + k y = F(t)$$

## Resilient-object



$$m_{eq} \frac{d^2 Func}{dt^2} + c_{eq} \frac{dFunc}{dt} + k_{eq} Func = de(t)$$

**Figure 2.** Analogy between a mass-spring-damper system and a resilient object.

The benefits of the jaw coupling become more apparent in a new requirement for a higher force  $P^{req}$  (Scenario 2). In this case, the existing motor cannot provide the required torque ( $T_2$ ) to meet the new  $P^{req}$ . As a result, a more powerful motor is installed. In Alternative A, the standardised interface simplifies the motor replacement but leads to unintended heat generation ( $q$ ), which affects gear teeth contact due to increased temperature. To counterbalance this effect, further changes, such as a new shaft or different gear, are necessary. In Alternative B, the jaw coupling absorbs the heat, allowing the system to adapt to the new requirements while maintaining the same structure. This approach offers advantages in terms of cost efficiency and sustainability.

### Modelling resilient objects and relation to margins

The jaw coupling example highlights the fundamental concept of resilient objects: they are versatile components integrated into a system to preserve its intended functionality in the face of various disruptive events. Simultaneously, they reduce the necessity to reconfigure the system to recover from such disruptions. To model the performance of resilient objects, we draw parallels with analogous existing systems, like car suspensions. A suspension system is often represented as a mass-spring-damper system (Figure 2), featuring a mass ( $m$ ) connected to a spring and a damper.

When an external force  $F$  is applied to the mass (e.g. due to a road bump), the object's position over time is determined by a second-order differential equation of motion. The system's ability to preserve its original position  $y(0)$  depends on two critical properties: the spring stiffness  $k$  and the damping coefficient  $c$ .

For resilient objects, we adopt a similar notation with some generalisations. The object's position  $y(t)$  corresponds to the generic functionality  $func(t)$  that must be sustained. The external force  $F$  is replaced by a generic disruptive event ( $de(t)$ ), representing a specific condition that degrades the system's functionality. Resilient objects prioritise absorbing

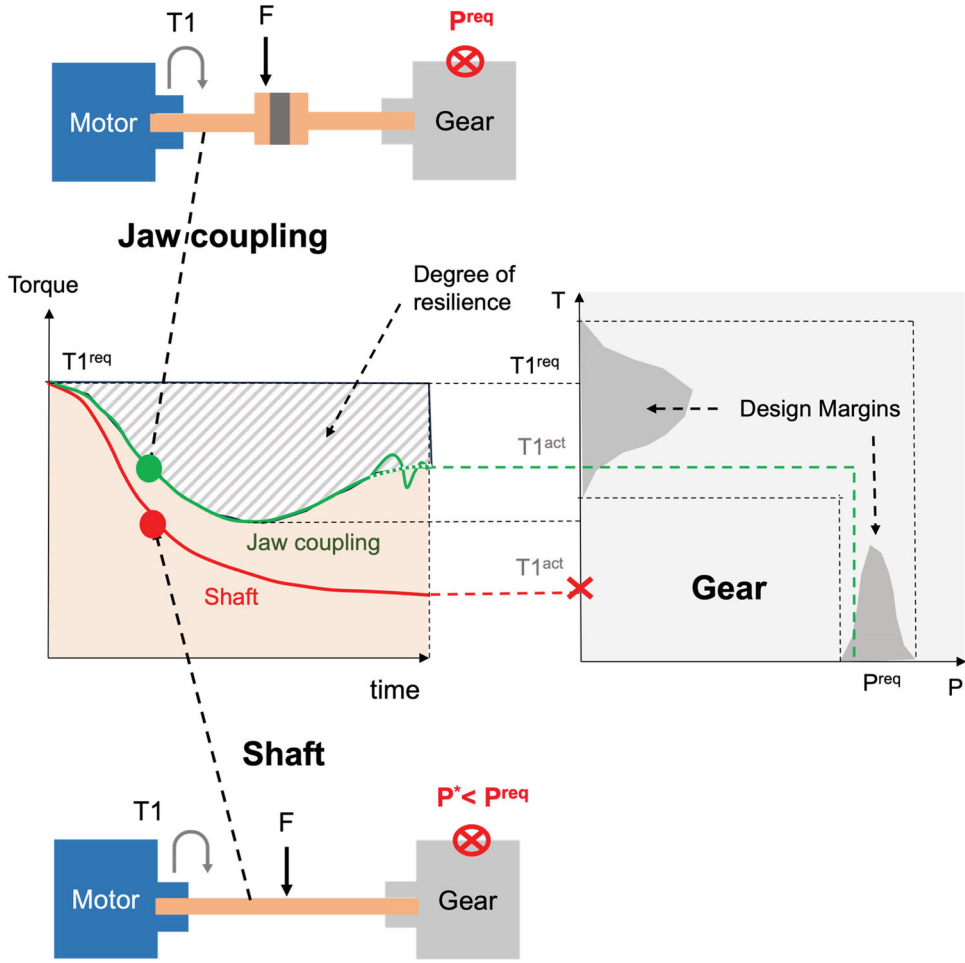


**Figure 3.** Relation between resilient objects and margins for a system (a) without a resilient object (single shaft) (b) with a resilient object (jaw coupling).

potential disruptive events to maintain system functionality. This ‘absorbing’ capability is inherent to the resilient object’s properties, here renamed as  $m_{eq}$ ,  $k_{eq}$  and  $c_{eq}$ . The governing equation is expressed as follows:

$$m_{eq} \frac{d^2 Func}{dt^2} + c_{eq} \frac{dFunc}{dt} + k_{eq} Func = de(t) \quad (1)$$

The generalisation presented in Equation 1 enables the application of mass-spring-damper principles, which are already prevalent in detailed mechanical design (e.g. Scarfogliero, Stefanini, and Dario 2009; Kurowski 2022), during the early design stages. especially when detailed system information is incomplete and subject to changes (Jarratt et al. 2011; Koh et al. 2015). Furthermore, it facilitates the analysis of resilient object performance in connection with margins. This relationship is illustrated in Figure 3, extending the jaw coupling example.

In the case of the single shaft (left graph, red line), prolonged misalignment reduces the delivered Torque ( $T^{act}$ ) at the gear contact (red cross point in the right graph). The gear was designed with margins to accommodate torque deviations while ensuring the desired force  $P^{eq}$  at the teeth contact. However, the misalignment exceeds allowable margins, necessitating redesign and replacement of either the shaft or gear. Notably, the torque from the shaft remains irreversibly altered even when the load  $F$  is removed over time. Conversely, the jaw coupling exhibits a different behaviour. Torque reduction is slower than the single shaft and can potentially return to acceptable levels if the load  $F$  decreases over time, signifying reversible misalignment. In this case, neither the gear nor the shafts require replacement. The shaded area between the required ( $T^{eq}$ ) and actual torque ( $T^{act}$ , green line) represents the resilient object's degree of resilience, similar to the 'resilience triangle' model (e.g. Tierney and Bruneau 2007; Koh 2022). It is worth noting also that the torque with the resilient object temporarily falls below allowable margins (lowest point of the green line). However, this brief loss of functionality is mitigated by the resilient object's ability to self-correct, occasionally resulting in oscillations (seen in the right part of the left graph). This limited loss of functionality may be motivated by business considerations to maintain system simplicity, as explored in the next section regarding the relationship between resilient objects, margins, and complexity.

Reading Figure 3, one could consider that since resilient objects are intended to be placed in areas that matter to avoid failure, such object may seem to relate more to reliability than resilience. Recognising that resilience and reliability are two connected concepts (Chalupnik, Wynn, and Clarkson 2013) this paper emphasises resilience rather than reliability for two reasons. The first is that in traditional reliability literature, systems are considered reliable if they have predictable performances in stable environments and stable requirements (Chalupnik, Wynn, and Clarkson 2013). As shown in Figure 3, resilient objects consider changes both in environment and requirements. The second reason is that traditional reliability engineering focuses on extending the point of failure in time by changing the structure. In Figure 3, this would be for example to increase the diameter of the shaft, so that  $T^{act}$  can be maintained stable and equal to  $T^{eq}$ . The resilient object instead, accepts partial loss of functionality and focuses on quickly recovering from it.

At the same time, the concept of resilient objects presented in this paper is focusing on recovering, but not so much on failure. Resilience is an acknowledgement that not all failures can be prevented (for example, because they are extremely rare; e.g. Brevault et al. 2016). In Figure 3, this would consider cases in which actions are taken from recovering from events that have brought the shaft to break. Hence, the need to bounce back is key. This paper recognises that the design of resilient object has not yet considered that not all failures can be prevented. Future work will be dedicated to considering such cases, with the objective to make resilient objects to fully embrace the notion of resilience.

### Relation to complexity

To assess complexity, this paper employs the structural complexity metric introduced by Sinha, Omer, and de Weck (2013), which has been previously validated in engineering design investigations (Sinha and de Weck 2016). The total structural complexity ( $C$ ) for a



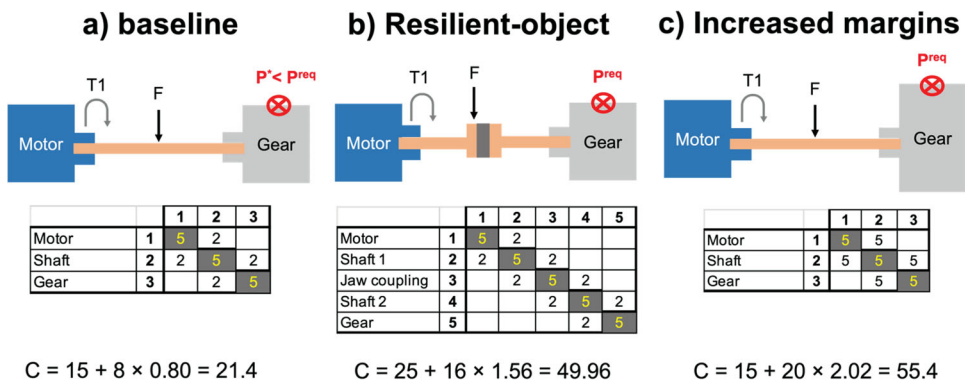


**Figure 4.** Impact on structural complexity (calculated following Sinha, Omer, and de Weck 2013) among (a) baseline (b) resilient object (c) baseline design with increased margins. The values on the diagonal of the matrix represent the individual complexity values, while the elements off-diagonal represent interface complexity values.

design is computed as follows:

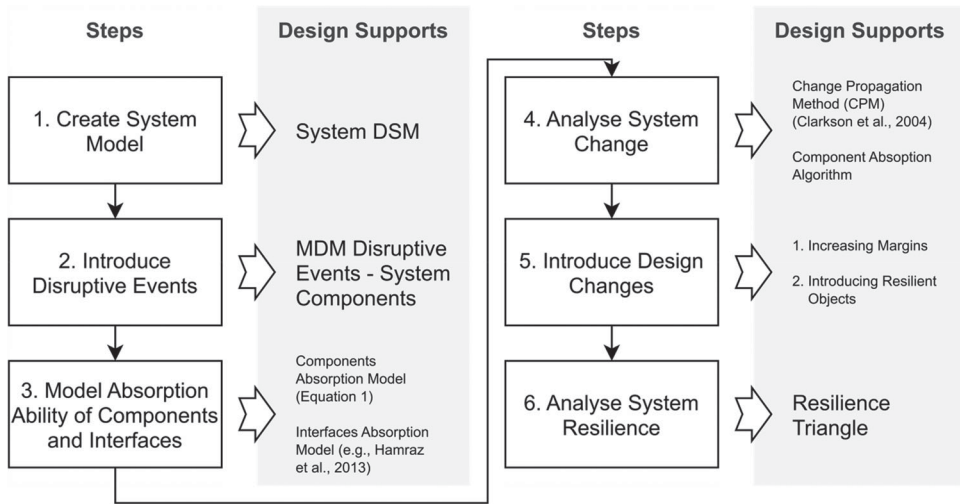
$$C = C_1 + C_2 \times C_3 \quad (2)$$

In this equation,  $C$  represents the overall system complexity, with  $C_1$  denoting individual component complexity,  $C_2$  representing complexity stemming from inter-component interactions, and  $C_3$  accounting for complexity due to component layout or architecture (called topological complexity). These complexity values can be obtained from historical component and interface data (Sinha and de Weck 2016).

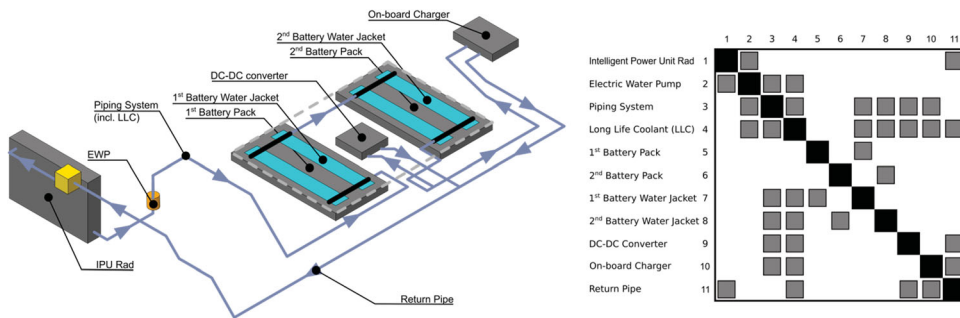
To illustrate complexity comparisons in the jaw coupling example, we present ‘ad-hoc’ values in Figure 4, intended only for conceptual presentation of alternatives and trade-offs.

Figure 4 demonstrates that the jaw coupling (b), in contrast to the baseline (a), offers protection from uncertainty but introduces increased component complexity (25 compared to 15 in the baseline) and higher interface complexity (16 compared to 8 in the baseline). The baseline design has lower total complexity (21.4 versus 49.96). However, it necessitates repair actions (Koh 2022) to rectify the system after misalignment, impacting process complexity. Thus, the jaw coupling introduces some overdesign but minimises repair actions. An alternative approach to protect the baseline system is to increase margins on the gear (c). This maintains the same individual complexity as the baseline (15). However, increased margins often result in higher interface complexity (Sinha and de Weck 2016), leading to elevated topological complexity, as determined by the singular value decomposition of the interface complexity matrix (Sinha, Omer, and de Weck 2013). This results in the highest overall complexity (55.4), potentially explaining the hidden overdesign often associated with systems with increased margins (Jones and Eckert 2023).

While this comparison relies on ‘ad-hoc’ values, it highlights the advantage of resilient objects in embedding resilience at the component level, reducing the risk of increasing topological complexity. Nonetheless, trade-offs exist in the ability of resilient objects to absorb uncertainty while maintaining lower complexity compared to other strategies, such as increasing margins in the design. The next section introduces an analytical method to explore these trade-offs.



**Figure 5.** The proposed method to analyse the impact of resilient objects.



**Figure 6.** Components and DSM of a cooling circuit in the Electric Powertrain for a battery electric vehicle (adapted from Yamagishi and Ishikura 2018). EWP = Electric Water Pump, RAD = Radiator, EWP = Electric Water Valve, IPU = Intelligent Power Unit.

## A method to analyse the impact of resilient objects

The method comprises six steps, as depicted in Figure 5, with each step offering various design support options that combine both new and existing methods.

These steps are implemented in an industrial application, specifically a cooling system for an electric powertrain in a Battery Electric Vehicle (BEV), adapted from Yamagishi and Ishikura (2018).

### Step 1: create system model

Figure 6 shows the 11 components and the Design Structure Matrix (DSM) of the cooling circuit (which represent the first design support used in the proposed method).

The cooling system is responsible for cooling two battery packs, a DC-DC converter, and the onboard charger. It utilises both an electric water pump (EWP) and a radiator (RAD)

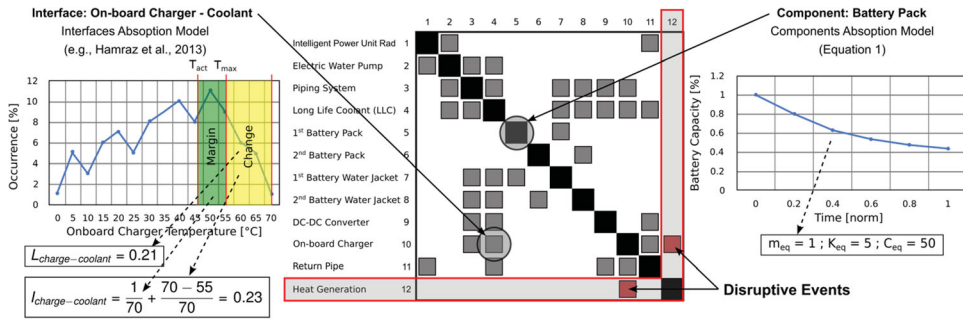


**Figure 7.** Model of the absorption ability of (A) interfaces (using interface data) and (B) components (adopting Equation 1 with estimated values for  $m_{\text{eq}}$ ,  $K_{\text{eq}}$  and  $C_{\text{eq}}$ ).

dedicated solely to the electric powertrain, positioned at the front of the vehicle. The battery cooling is achieved by circulating long-life coolant (LLC) through water jackets. After cooling, the coolant returns to the radiator via a return pipe. This system serves as the 'base-line' for analyzing the effects of disruptive events and design changes using the proposed method.

### Step 2: introduce disruptive events

This step involves adding disruptive events as new rows and columns in the system DSM, resulting in a Multi-Domain Matrix (MDM) following Eppinger and Browning (2012). In this example, only one disruptive event is considered, based on the empirical industrial evidence from Yamagishi and Ishikura (2018). The chosen disruptive event is the heat generation caused by the on-board charger during the charging phase. Charging, particularly with a more powerful charger, generates a significant amount of heat. Consequently, the MDM matrix (depicted in Figure 7 below) includes a dependency between the onboard charger and heat generation, representing the disruptive event.

### Step 3: model absorption ability of components and interfaces

As explained in Chapter 2, this paper considers that a system's capacity to handle uncertainty without requiring 'changes' (or restructuring) is determined by two factors:

1. The capacity of margins to absorb disruptive events at the interfaces between components, thereby preventing change propagation (Eckert, Clarkson, and Zanker 2004).
2. The intrinsic ability of the component itself to absorb or 'bounce back' from disruptive events, indicating its resilience as a resilient object.

This step involves modeling these two abilities, utilising two distinct models: one for interfaces and one for components. Figure 7 provides an example of a model applied to an interface (between the on-board charger and the long-life coolant) and one for a component (the batteries).

For interfaces (the off-diagonal elements in the MDM shown in Figure 7), the likelihood (L) and impact (I) of change between a component and its interfacing components are determined based on existing research on margins and change absorption (Hamraz et al. 2013). Other methods, such as the Margin Value Method (Brahma and Wynn 2020), can also be applied. Figure 7 (part A) shows an example of how L-I values at the on-board charger-coolant interface are derived from interface data (adapted from Ohgaki, Matsuda, and Matsumoto 2018). The model assumes a current on-board charger temperature of 45°C with a maximum allowable temperature of 55°C (a 10°C margin). The estimated likelihood of change beyond the maximum allowable temperature is 21%, while the estimated impact of this change is 23%, considering a minimal impact due to the margin and a major impact beyond the allowable temperature. Detailed calculations can be found in Hamraz et al. (2013).

For components (the diagonal elements in the MDM shown in Figure 7), Equation 1 (introduced in Chapter 2) is employed to describe their ability to maintain functionality when subjected to external disruptive events. This model relies on three parameters: the mass equivalent ( $m_{eq}$ ), stiffness equivalent ( $k_{eq}$ ), and damping coefficient equivalent ( $c_{eq}$ ). Historical data or experience can be used to estimate these values. Figure 7 (part B) illustrates the modeling of the battery packs' capacity degradation. In this case, the degradation is assumed to be over-damped, and the battery capacity does not recover over time when subjected to disruptive events (e.g. wear).

The derivation of  $k_{eq}$  and  $c_{eq}$  values involves normalising the time scale of degradation (0-1), setting  $m_{eq}$  to 1, specifying the wear impact ( $de = 0.2$ ), establishing the initial battery capacity ( $func = 100\%$ ) at  $t = 0$ , and the final battery capacity ( $func = 60\%$ ) at  $t = 1$ . By computer experimentation with  $k_{eq}$  and  $c_{eq}$  values and solving Equation 1, the final values can be determined (e.g.  $k_{eq} = 5$  and  $c_{eq} = 50$ ).

#### Step 4: analyse system change

To execute this step, the method employs a modified version of the Change Propagation Method algorithm (CPM; Clarkson, Simons, and Eckert 2004), which incorporates the components' absorption capabilities determined by  $m_{eq}$ ,  $k_{eq}$ , and  $c_{eq}$  values. The relevant variables for this algorithm are listed in Table 1, and a pseudo-code representation of the algorithm is provided in Table 2.

Figure 8 displays the outcomes of the implemented algorithm on the cooling system (baseline system). To simulate a disruptive event (heat generation) in line with industrial practice (Yamagishi and Ishikura 2018), high likelihood (L) and impact (I) values have been assigned to the interface (i.e. L-I  $de_{heat-ob-boardcharger} = 0.7$ ). In contrast, the L-I values for all other interfaces have been determined using the modified CPM algorithm (Table 2) and propagated four times to account for fourth-order effects.

Figure 8 indicates substantial disruptions in the baseline system results, resulting in a total risk score of 0.43. This perturbation is primarily attributed to the close connections between the battery packs and the onboard charger, facilitated by the piping system, coolant circulation, and return pipe. This scenario mirrors practical challenges, as batteries generate most heat during vehicle operation, while the onboard charger becomes the primary heat source when the vehicle is charging. When all components share the same cooling channel, the charger's heat generation during charging can elevate the battery

**Table 1.** Summary of model and elements of the proposed algorithm.

Element	Description
<code>n_components</code>	Represents the number of components in the system, which is set to 11 in this specific case.
<code>n_disr_events</code>	Indicates the number of disruption events or iterations the algorithm will perform. In this case, it is set to 1, meaning there is only one disruption event (heat generation).
Arrays <code>c1, k1, m1, F1</code>	These arrays store properties of the system's components, specifically: <code>c1</code> : Damping equivalent constants for each component. <code>k1</code> : Spring equivalent stiffness values for each component. <code>m1</code> : Mass equivalent values for each component (normalized and $= 1$ ). <code>F1</code> : disruptive events acting on each component.
<code>design_structure</code>	A matrix that represents the design structure of the system. It defines how components are interconnected and the relationships between them.
<code>df_margins</code>	A matrix representing the margin values associated with the interfaces (dependencies) in design structure. Margins are typically used to measure the robustness or reliability of the system components.
<code>df_req</code>	A matrix representing the requirement values associated with the interfaces (dependencies) in the design structure. These requirements specify what the system should achieve.
<code>tstart, tstop, increment</code>	Parameters for setting the time span and increment used for simulation. <code>tstart</code> is the start time, <code>tstop</code> is the end time, and <code>increment</code> is the time step.
<code>x_init</code>	An array that represents the initial conditions of the system components, typically used for time integration.
<code>T</code>	An array used to define a time grid for simulation.
<code>n_steps</code>	An integer value that determines the number of iterations in the main CPM algorithm. It controls how many times the algorithm will update the system.

temperature, leading to battery degradation (Yamagishi and Ishikura 2018). The degradation is evident in the diagonal elements of the DSM matrix, representing component absorption capability (each diagonal element shows the graph depicting the solution to Equation 1 integrated over time). This capability depends on  $m_{eq}$ ,  $k_{eq}$ , and  $c_{eq}$  values. For this instance, low  $m_{eq}$ ,  $k_{eq}$ , and  $c_{eq}$  values are assigned to the battery packs, reflecting a high sensitivity of battery capacity to the disruptive event (heat generation). In contrast, other elements like the pump have higher  $m_{eq}$ ,  $k_{eq}$ , and  $c_{eq}$  values, indicating reduced sensitivity to heat and a lower likelihood of propagating changes to interfacing elements.

To counteract battery degradation, designers can employ two strategies: (1) enhancing margins at interfaces with connecting components to enable heat absorption by the interface, or (2) introducing resilient objects capable of absorbing heat. The subsequent section delves into the consequences of these strategies.

### **Step 5: introduce design changes: managing margins vs. using resilient objects**

The first alternative (a) entails increasing margins by introducing a higher-grade coolant. This adjustment enables the absorption of heat propagation from the onboard charger, effectively shifting the margin and requirements to the right side of Figure 7. Consequently, it reduces the likelihood and impact on all components interfacing with the coolant, such as the cooling jackets. This approach positively impacts system resilience, as illustrated in Figure 9. It mitigates the propagation chain within the system, resulting in a total risk score of 0.19. However, it may pose a risk of overdesigning the system, potentially necessitating a redesign of elements like the piping system to accommodate the higher-grade coolant.

**Table 2.** Proposed algorithm, adapting the benefit of resilient objects to margins and the CPM algorithm.

---

**Pseudocode for the Proposed Algorithm**

---

```

# 1. Variable Initialization
n_components = 11
n_disr_events = 1
# Initializing arrays for system's component properties
c1 = [] # Damping equivalent constants for each component
k1 = [] # Spring equivalent stiffness values for each component
m1 = [] # Mass equivalent values for each component (normalized to 1)
F1 = [] # Disruptive events acting on each component
# 2. Load Design Matrices
# Load matrices from external sources and assign them
design_structure = load_matrix("design_structure_file.csv")
df_margins = load_matrix("df_margins_file.csv")
df_req = load_matrix("df_req_file.csv")
# 3. Simulation Parameters
tstart = 0 # Start time
tstop = 0 # End time
increment = 0 # Time step
x_init = [] # Initial conditions array
t = [] # Time grid array for simulation
# 4. Direct Likelihood and Impact Calculation
def calculate_likelihood_impact(interface, design_structure, df_margins,
    df_req):
    # Implementation of the function to calculate likelihood and impact
    pass
# Loop through interfaces and calculate likelihood and impact
for interface in design_structure:
    calculate_likelihood_impact(interface, design_structure, df_margins,
        df_req)
# 5. Main Algorithm
n_steps = 0 # Number of iterations for the CPM algorithm
for event in range(n_disr_events): # For each disruption event
    for i in range(n_components): # Iterate through components
        # Update disruptive events based on design structure
        update_disruptive_events(i, design_structure)
        # Calculate and solve differential equation for new state
        new_state = solve_differential_equation(i)
        # Update design structure with new state values
        design_structure[i][i] = new_state
        # Calculate direct likelihood and impact
        calculate_likelihood_impact(i, design_structure, df_margins, df_req)
        # Run CPM and calculate combined matrices
        run_CPM_calculations(design_structure, n_steps)
        # Update design structure with new risk values
        update_design_structure_with_risk(design_structure)
# 6. End of the Algorithm

```

---

Additionally, maintaining a connection between the onboard charger and the batteries through the cooling channel makes the system non-resilient to further increases in battery pack and onboard charger capacity. When the impact of heat generation is heightened to 0.9, the total risk of this system increases to 0.49. This results from the heat generated exceeding the margin allowed by the higher-grade coolant, thereby propagating the change to interfacing elements. To mitigate this effect, an even higher-grade coolant should be utilised.

Alternatively (b), to prevent the flow of heated coolant from the onboard charger to the battery, one or more 'resilient objects' can be inserted (Figure 10-b). In this case, it involves

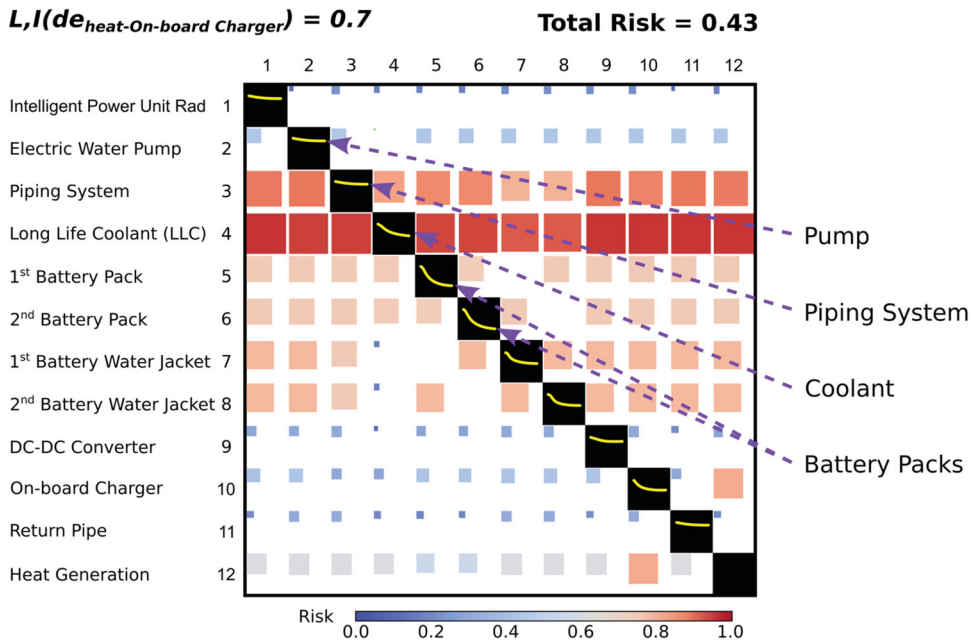


**Figure 8.** Impact of change propagation on baseline system with an initiated disruptive event (on-board charger generating heat) with likelihood and impact = 0.7 (scale 0–1). The graphs in the diagonal elements of the DSM show to absorption ability of the single components (given by  $m_{eq}$ ,  $k_{eq}$  and  $c_{eq}$ ).

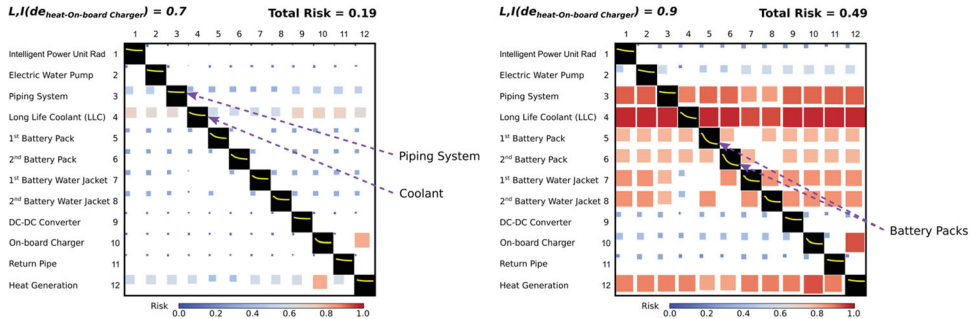


**Figure 9.** Impact of change propagation on baseline system with increased margins (through the insertion of a higher-grade coolant).

the insertion of an Electric Water Valve (EWW) and a bypass water channel that switches coolant circuits when the coolant's temperature exceeds that of the battery. These solutions align with the approach taken by Yamagishi and Ishikura (2018).

The action of these two resilient objects on the system is dual in nature. First, they eliminate the connection between the onboard charger and the batteries through the cooling channel. Rising temperatures are averted by rerouting the coolant through the bypass circuit when the coolant temperature surpasses that of the batteries. Second, these two components exhibit the capability to remain resilient even in the face of further increases in heat generated by the onboard charger. When switched, they completely remove the



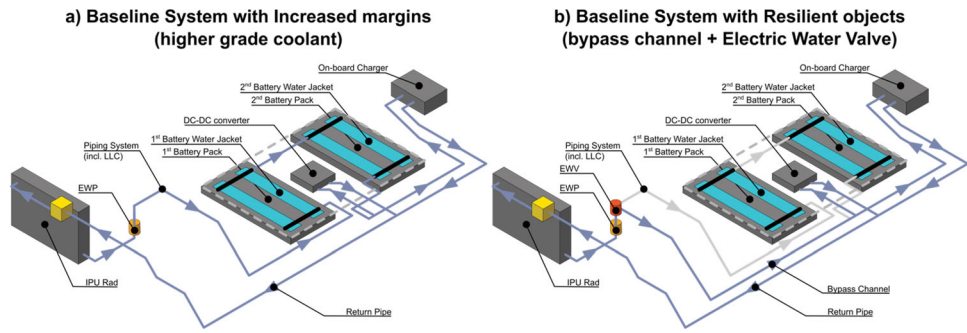


**Figure 10.** Alternative designs considered (a) baseline system with increased margins (higher grade coolant) and (b) a baseline system with resilient objects (a bypass channel with an electric valve).

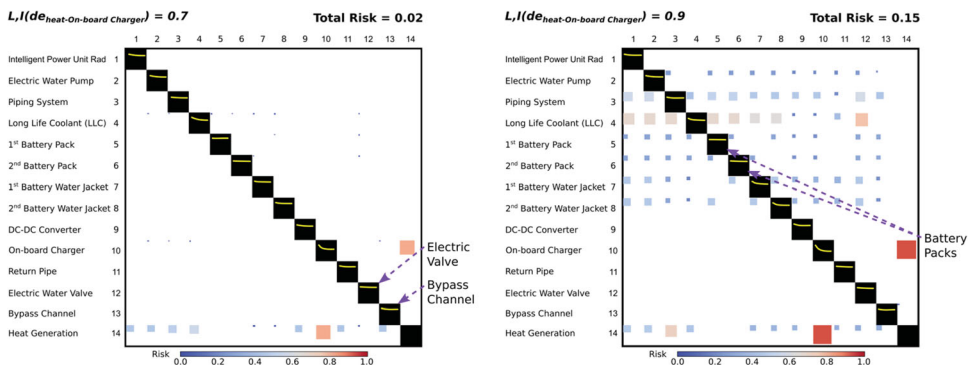


**Figure 11.** Impact of change propagation on baseline system with resilient objects.

interaction between the coolant and the water jackets. This resilience is achieved by assigning high values to  $k_{eq}$  and  $c_{eq}$  ( $k_{eq} = 10$ ,  $c_{eq} = 20$ ). The impact of these two resilient objects is evident in Figure 11: as heat generation increases from 0.7 to 0.9, the total risk rises only slightly (0.15), which is lower than the increase observed in the baseline system when using a higher-grade coolant.

The insertion of resilient objects has enabled us to keep the baseline system with its (lower) original margins. Furthermore, these margins provided by the coolant could be further relaxed, for instance by reducing the amount of water used in the cooling system. This is achievable due to the absorption capability provided by the Electric Water Valve (EWW) and the bypass channel, as demonstrated in the graphs in the diagonal elements. Incorporating the EWW and the bypass could simplify various system components, such as reducing the quantity of coolant used and employing lower-grade materials for hoses in the piping system. This streamlining has a positive impact on the cost-efficiency and environmental sustainability of the system.

The degree of resilience in these three systems can be assessed using an approach similar to that of Tierney and Bruneau (2007) and Koh (2022). It involves calculating the integral area above the absorption graphs in the diagonal of the DSM, as shown in Figure 11. This enables a comparison of the resilience embedded in these systems against their complexity (Step 6), using metrics such as those proposed by Sinha, Omer, and de Weck (2013). The



subsequent section will provide a more detailed exploration of the theoretical and practical implications of this research, as well as its limitations.

## Discussion

The examples of resilient objects presented in this paper (e.g. jaw coupling, EWV, and bypass) demonstrate their utility in managing disruptive events within an engineering system. Current literature often prioritises coping with disruptive events by emphasising system changeability (e.g. Otto et al. 2016) or rapid recovery and repair (e.g. Koh 2022). While this paper acknowledges the benefits of these approaches, it highlights their resource consumption, potentially impacting cost efficiency and sustainability. Consequently, resilient objects offer a strategy of ‘passive protection’ against uncertainty instead (Chalupnik, Wynn, and Clarkson 2013) by absorbing uncertainties without necessitating system alterations. Similar objectives are pursued by margin-focused research (e.g. Eckert, Isaksson, and Earl 2019; Brahma and Wynn 2020; Brahma, Wynn, and Isaksson 2022; Jacobson and Ferguson 2023; Brahma et al. 2023), which advocates for the careful definition of buffers and excess at interfaces to interrupt the propagation of change triggered by disruptions. While this approach offers benefits, it often involves hidden overdesign (e.g. Jones and Eckert 2023). Consequently, the positive over-capacity provided by margins frequently requires trade-offs considering the additional cost and complexity in the system (Jones, Eckert, and Gericke 2018; Jones, Eckert, and Garthwaite 2020). This paper has proposed a way to solve such trade-offs, by looking at the components of the system themselves, rather than at the interfaces. The core idea with resilient objects is that resilience is embedded locally in the regions of the system that are most susceptible to uncertain conditions. This is achieved in two ways. First, disruptive events are confined by altering the system’s topology. For example, in the cooling system case, the connection between the onboard charger and the batteries through the cooling channel was removed, eliminating the need for margins. This approach allows for the application of axiomatic design principles (Suh 1995) to margins and resilience. Second, the absorption capability depends on the intrinsic design properties of the resilient objects, characterised by  $m_{eq}$ ,  $k_{eq}$ , and  $c_{eq}$ . Introducing resilient objects can potentially remove or reduce interface margins, thereby minimising the risk for system over-design. However, the incorporation of resilient objects may introduce some level of local over-design at the component level (e.g. the addition of the EWV and the bypass channel). Therefore, the choice of strategy remains context-dependent. Future research will investigate the trade-off between resilience and complexity by comparing strategies that emphasise increasing design margins with those focusing on resilient objects. This will enable budgeting for resilience, in alignment with recommendations from current complexity research (Sinha, Suh, and de Weck 2018).

In contrast to existing literature on margins, this paper introduces a temporal dimension. Historically, a system’s ability to absorb disruptive events has been viewed as ‘static’ over time, determined by the initial specifications and margins incorporated during design (Eckert, Clarkson, and Zanker 2004). These margins are often considered as ‘consumed’ or ‘used up’ throughout the system’s history as changes occur (Eckert, Clarkson, and Zanker 2004, 19). Section 2.2 (e.g. Figure 3) introduces the concept of ‘dynamic margins,’ where a system’s ability to absorb disruptive events is influenced by both the intrinsic ‘absorbing’ capabilities of its components ( $m_{eq}$ ,  $k_{eq}$ , and  $c_{eq}$ ) and the magnitude and duration of the

disruptive event ( $de(t)$ ). This means that margins may not always be ‘used up’ over time. In certain situations, when a disruptive event is of short duration and moderate magnitude, and the system incorporates well-designed resilient objects, the system’s capability can return within acceptable margins, even achieving full resilience. This has favourable implications for the cost-efficiency and sustainability of the system.

In Section 3, the cooling system case study demonstrates the practical application of resilient objects, particularly in absorbing heat generated by the on-board charger. However, it is intriguing to consider various disruptive events beyond heat generation.

An approach introduced by Panarotto et al. (2023) employs a Design of Experiments and design automation methodology, inspired by the work proposed by Colombo, Cascini, and de Weck (2015). For resilience analysis, generic disruptive events are systematically introduced one by one as new rows and columns in the system’s DSM, creating a structure similar to the one presented in Figure 7. This approach aims to replicate the realistic non-linear behaviour observed in mechanical systems (e.g. Missoum 2007), where a disruptive event results from the interaction with another disruptive event within the system. Through repeated simulations with randomly assigned L-I values, multiple MDMs are generated, and the cumulative impact can be assessed to determine if there is a minimum number of disruptive events that triggers uncontrolled propagation in the system. Nevertheless, the sensitivity of this Design of Experiments approach requires further exploration and remains a subject for future work. For instance, there may be cases where disruptive events comprise multiple sub-disruptive events, introducing variations due to differing levels of abstraction in the analysis. Achieving consistency in describing disruptive events and implementing normalisation at appropriate stages are areas of investigation in future research.

The design of resilient objects remains a topic for future research. Existing studies (Panarotto et al. 2023) have explored resilient object design using a text mining approach to extract general-purpose design principles for addressing various disruptive events, such as heat generation and electromagnetic interference. Combining these solutions in a morphological matrix can serve as an initial source of inspiration for general-purpose resilient objects. However, a limitation of the morphological matrix approach is that it does not consider specific interactions between solutions, as it primarily focuses on individual components. This approach may lead to overdesigned solutions compared to a more holistic methodology.

## Conclusion

In an era of increasing uncertainties in both market and technology, traditional approaches to product development are being challenged. This paper has introduced the concept of ‘resilient objects’ as a means to passively protect systems from disruptive events and uncertainties. Resilient objects are strategically integrated into products, allowing them to absorb a wide range of uncertainties without the need for extensive changes or complex margins at interfaces.

The study has illustrated the effectiveness of resilient objects using practical examples, showing how they can maintain system functionality when subjected to disruptive events of different kinds. The analysis has also highlighted the trade-offs between resilience and complexity, emphasising the potential benefits of designing resilience at the component level.

This paper opens new avenues for research into the design of resilient objects and their impact on system design and complexity. The dynamic perspective on margins and time-dependent resilience provides valuable insights for engineering and product development, offering the potential to improve cost efficiency and sustainability in the face of evolving uncertainties. Future work will explore and quantify these trade-offs in more specific contexts.

## Disclosure statement

No potential conflict of interest was reported by the author(s).

## Funding

This work was supported by VINNOVA: [Grant Number 2018-02692].

## ORCID

Massimo Panarotto  <http://orcid.org/0000-0001-5216-0944>

Iñigo Alonso Fernández  <http://orcid.org/0000-0003-3991-1939>

## References

- Brahma, A., S. Ferguson, C. Eckert, and O. Isaksson. 2023. "Margins in Design – Review of Related Concepts and Methods." *Journal of Engineering Design*, 1–34. <https://doi.org/10.1080/09544828.2023.2225842>.
- Brahma, A., and D. C. Wynn. 2020. "Margin Value Method for Engineering Design Improvement." *Research in Engineering Design* 31 (3): 353–381. <https://doi.org/10.1007/s00163-020-00335-8>.
- Brahma, A., D. Wynn, and O. Isaksson. 2022. "Use of Margin to Absorb Variation in Design Specifications: An Analysis Using the Margin Value Method." *Proceedings of the Design Society* 2: 323–332. <https://doi.org/10.1017/pds.2022.34>.
- Brevault, L., S. Lacaze, M. Balesdent, and S. Missoum. 2016. "Reliability Analysis in the Presence of Aleatory and Epistemic Uncertainties, Application to the Prediction of a Launch Vehicle Fallout Zone." *Journal of Mechanical Design* 138 (11): 111401. <https://doi.org/10.1115/1.4034106>.
- Chalupnik, M. J., D. C. Wynn, and P. J. Clarkson. 2013. "Comparison of Ilities for Protection Against Uncertainty in System Design." *Journal of Engineering Design* 24 (12): 814–829. <https://doi.org/10.1080/09544828.2013.851783>.
- Christopher, M., and C. Rutherford. 2004. "Creating Supply Chain Resilience Through Agile Six Sigma." *Critical eye* 7 (1): 24–28.
- Clarkson, P. J., C. Simons, and C. Eckert. 2004. "Predicting Change Propagation in Complex Design." *Journal of Mechanical Design* 126 (5): 788–797. <https://doi.org/10.1115/1.1765117>.
- Colombo, E. F., Cascini, G., & de Weck, O. L. (2015). Impact of Architecture Types and Degree of Modularity on Change Propagation Indices. In *DS 80-3 Proceedings of the 20th International Conference on Engineering Design (ICED 15) Vol 3: Organisation and Management*, Milan, Italy, 27-30.07, 187–198.
- Cross, N. 2006. *Designersly Ways of Knowing*, 1–13. Springer London.
- De Neufville, R., and S. Scholtes. 2011. *Flexibility in Engineering Design*. MIT Press.
- Eckert, C., P. J. Clarkson, and W. Zanker. 2004. "Change and Customisation in Complex Engineering Domains." *Research in Engineering Design* 15: 1–21. <https://doi.org/10.1007/s00163-003-0031-7>.
- Eckert, C., O. Isaksson, and C. Earl. 2019. "Design Margins: A Hidden Issue in Industry." *Design Science* 5. <https://doi.org/10.1017/dsj.2019.7>.
- Eckert, C., O. Isaksson, S. Hallstedt, J. Malmqvist, AÖ Rönnbäck, and M. Panarotto. 2019, July. Industry Trends to 2040. In *Proceedings of the Design Society: International Conference on Engineering Design (Vol. 1, No. 1, pp. 2121–2128)*. Cambridge University Press.

- Eppinger, S. D., and T. R. Browning. 2012. *Design Structure Matrix Methods and Applications*. MIT Press.
- Guo, X., M. Yang, Y. Liu, W. Zhao, J. Shi, and K. Zhang. 2023. "Design for Product Resilience: Concept, Characteristics and Generalisation." *Journal of Engineering Design*, 1–20.
- Hamraz, B., O. Hisarciklilar, K. Rahmani, D. C. Wynn, V. Thomson, and P. J. Clarkson. 2013. "Change Prediction Using Interface Data." *Concurrent Engineering* 21 (2): 141–154. <https://doi.org/10.1177/1063293X13482473>.
- Hollnagel, E., C. P. Nemeth, and S. Dekker. 2008. *Resilience Engineering Perspectives: Remaining Sensitive to the Possibility of Failure (Vol. 1)*. Ashgate Publishing, Ltd.
- Hosseini, S., K. Barker, and J. E. Ramirez-Marquez. 2016. "A Review of Definitions and Measures of System Resilience." *Reliability Engineering & System Safety* 145: 47–61. <https://doi.org/10.1016/j.res.2015.08.006>.
- Jacobson, L., and S. Ferguson. 2023. "A Hierarchical Exploration of How Design Margins Enable Adaptability." *Proceedings of the Design Society* 3: 191–200. <https://doi.org/10.1017/pds.2023.20>.
- Jarratt, T. A. W., C. M. Eckert, N. H. Caldwell, and P. J. Clarkson. 2011. "Engineering Change: An Overview and Perspective on the Literature." *Research in Engineering Design* 22 (2): 103–124. <https://doi.org/10.1007/s00163-010-0097-y>.
- Jones, D., and C. Eckert. 2023. "Hidden Overdesign in Building Services: Insights from Two UK Hospital Case Studies." *Journal of Engineering Design* 34 (7): 437–461. <https://doi.org/10.1080/09544828.2023.2231156>.
- Jones, D. A., C. Eckert, and P. Garthwaite. 2020, May. "Managing Margins: Overdesign in Hospital Building Services." In *Proceedings of the Design Society: DESIGN Conference* (Vol. 1, pp. 215–224). Cambridge University Press.
- Jones, D. A., C. M. Eckert, and K. Gericke. 2018. "Margins Leading to Over-Capacity." In DS 92: *Proceedings of the DESIGN 2018 15th International Design Conference*, 781–792.
- Jones, J., L. Warrington, and N. Davis. 2001, January. "The Use of a Discrete Event Simulation to Model the Achievement of Maintenance Free Operating Time for Aerospace Systems." In *Annual Reliability and Maintainability Symposium. 2001 Proceedings. International Symposium on Product Quality and Integrity (Cat. No. 01CH37179)*, 170–175. IEEE.
- Koh, E. C. 2022. "Resilience Analysis of Infrastructure Systems in Incremental Design Change." *Computers in Industry* 142: 103734. <https://doi.org/10.1016/j.compind.2022.103734>.
- Koh, E. C., A. Förg, M. Kreimeyer, and M. Lienkamp. 2015. "Using Engineering Change Forecast to Prioritise Component Modularisation." *Research in Engineering Design* 26: 337–353. <https://doi.org/10.1007/s00163-015-0200-5>.
- Kurowski, P. M. 2022. *Finite Element Analysis for Design Engineers*. SAE International.
- Missoum, S. 2007. "Controlling Structural Failure Modes During an Impact in the Presence of Uncertainties." *Structural and Multidisciplinary Optimization* 34: 463–472. <https://doi.org/10.1007/s00158-007-0100-z>.
- Ohgaki, T., M. Matsuda, and M. Matsumoto. 2018. *Integrated Cooling System for Underfloor High Voltage Devices in PHEV (No. 2018-01-1184)*. SAE Technical Paper.
- Otto, K., K. Hölttä-Otto, T. W. Simpson, D. Krause, S. Ripperda, and S. Ki Moon. 2016. "Global Views on Modular Design Research: Linking Alternative Methods to Support Modular Product Family Concept Development." *Journal of Mechanical Design* 138 (7): 071101. <https://doi.org/10.1115/1.4033654>.
- Panarotto, M., V. Giordano, F. Chiarello, A. Brahma, I. A. Fernández, and G. Fantoni. 2023. "Text Mining of Resilient Objects Absorbing Change and Uncertainty." *Proceedings of the Design Society* 3: 3325–3334. <https://doi.org/10.1017/pds.2023.333>.
- Scarfogliero, U., C. Stefanini, and P. Dario. 2009. "The Use of Compliant Joints and Elastic Energy Storage in Bio-Inspired Legged Robots." *Mechanism and Machine Theory* 44 (3): 580–590. <https://doi.org/10.1016/j.mechmachtheory.2008.08.010>.
- Sinha, K., and O. L. de Weck. 2016. "Empirical Validation of Structural Complexity Metric and Complexity Management for Engineering Systems." *Systems Engineering* 19 (3): 193–206. <https://doi.org/10.1002/sys.21356>.

- Sinha, K., H. Omer, and O. L. de Weck. 2013. "Structural Complexity: Quantification, Validation and its Systemic Implications for Engineered Complex Systems." In *DS 75-4: Proceedings of the 19th International Conference on Engineering Design (ICED13)*, 189–198.
- Sinha, K., E. S. Suh, and O. de Weck. 2018. "Integrative Complexity: An Alternative Measure for System Modularity." *Journal of Mechanical Design* 140 (5): 051101. <https://doi.org/10.1115/1.4039119>.
- Stahel, W. R. 2016. "The Circular Economy." *Nature* 531 (7595): 435–438. <https://doi.org/10.1038/531435a>.
- Suh, N. P. 1995. "Axiomatic Design of Mechanical Systems." *Journal of Mechanical Design* 117 (B): 2–10. <https://doi.org/10.1115/1.2836467>.
- Suh, E. S., M. R. Furst, K. J. Mihalyov, and O. D. de Weck. 2010. "Technology Infusion for Complex Systems: A Framework and Case Study." *Systems Engineering* 13 (2): 186–203. <https://doi.org/10.1002/sys.20142>.
- Tierney, K., and M. Bruneau. 2007. *Conceptualizing and Measuring Resilience: A Key to Disaster Loss Reduction*. TR news (250).
- Uday, P., and K. Marais. 2015. "Designing Resilient Systems-of-Systems: A Survey of Metrics, Methods, and Challenges." *Systems Engineering* 18 (5): 491–510. <https://doi.org/10.1002/sys.21325>.
- Ulrich, K. 1995. "The Role of Product Architecture in the Manufacturing Firm." *Research Policy* 24 (3): 419–440. [https://doi.org/10.1016/0048-7333\(94\)00775-3](https://doi.org/10.1016/0048-7333(94)00775-3).
- Wied, M., J. Oehmen, and T. Welo. 2020. "Conceptualizing Resilience in Engineering Systems: An Analysis of the Literature." *Systems Engineering* 23 (1): 3–13. <https://doi.org/10.1002/sys.21491>.
- Yamagishi, T., and T. Ishikura. 2018. "Development of Electric Powertrain for Clarity Plug-In Hybrid." *SAE International Journal of Alternative Powertrains* 7 (3): 323–334.
- Yodo, N., and P. Wang. 2016. "Engineering Resilience Quantification and System Design Implications: A Literature Survey." *Journal of Mechanical Design* 138 (11): 111408. <https://doi.org/10.1115/1.4034223>.
- Zimmermann, M., S. Königs, C. Niemeyer, J. Fender, C. Zeherbauer, R. Vitale, and M. Wahle. 2017. "On the Design of Large Systems Subject to Uncertainty." *Journal of Engineering Design* 28 (4): 233–254. <https://doi.org/10.1080/09544828.2017.1303664>.